RSC Advances

ROYAL SOCIETY OF CHEMISTRY

PAPER

View Article Online
View Journal | View Issue

Cite this: *RSC Adv.*, 2022, **12**, 3897

Comprehensive profiling of *Platycodonis radix* in different growing regions using liquid chromatography coupled with mass spectrometry: from metabolome and lipidome aspects†

Weizhen Huang,‡[ab] Lan Lan,‡[b] Heng Zhou,[b] Jiajia Yuan,[b] Shui miao,[b] Xiuhong Mao,[b] Qing Hu[b] and Shen Ji*[b]

Received 11th November 2021
Accepted 22nd January 2022

DOI: 10.1039/d1ra08285j

rsc.li/rsc-advances

Platycodon grandiflorus (Jacq.) A. DC. is widely cultivated across the south and north of China. Its root, *Platycodonis radix*, is commonly used as a vegetable, functional food, and traditional herbal medicine with various biological benefits. It is critical to fully clarify the chemical composition of *Platycodonis radix* for the sake of the food industry and traditional herb markets. In this study, a strategy of metabolome and lipidome profiling based on ultra-high performance liquid chromatography coupled to ion mobility-quadrupole time of flight mass spectrometry (UPLC-IM-QTOF-MS) was developed to reveal the overall chemical composition of *Platycodonis radix*. IN particular, comprehensive lipidome profiling was first performed for *Platycodonis radix*, in which 170 lipid molecular species including 55.9% glycerophospholipids, 31.2% glycerolipids, and 12.9% sphingolipids were identified. *Platycodonis radix* from two major production regions in China, Inner Mongolia and Anhui province, were collected and analyzed by the MS based approach combined with multivariate statistical analysis from both the metabolome and lipidome aspects. This study threw focus on the profiling investigations of *Platycodonis radix* from different growing regions and provided new potential in the lipidome analysis of medicinal food.

1. Introduction

Platycodon grandiflorus (Jacq.) A. DC. is a herbaceous perennial that belongs to the genus *Platycodon* of the Campanulaceae family. *Platycodonis radix*, the dried whole root of *Platycodon grandiflorus* (Jacq.) A. DC., is widely applied for its therapeutic effects towards coughs, phlegm, sore throat and other pulmonary or respiratory disorders as a traditional herbal medicine in many Asian countries, and thus is an important ingredient in clinical bronchitis and tonsillitis relief preparations.[1,2] It is also consumed as a functional food with various nutrients in the northeast of China, Korea and Japan. It can be processed into preserved fruit, health drinks and noodles in the modern food industry. Cosmetic addition is also a burgeoning use in recent years.[3] *Platycodonis radix* is rich in triterpenoid saponins, flavonoids, phenolic acids, polyacetylenes, and polysaccharides.[4,5] Previous studies have shown that *Platycodonis radix* exhibits various pharmacological properties such as apophlegmatic, anti-inflammatory, anti-cancer, anti-obesity, anti-diabetic, immunomodulatory, cardiovascular protective and hepatoprotective activities.[5–8] With its increasing consumption, cultivated *Platycodonis radix* has become an alternative to the wild variety over the years. At present, the output in a normal year in China is 1 million kg, of which export accounts for half.[3] Interest in assessing and elaborating the chemical profile of *Platycodonis radix* has been growing.

Different growth environment and pattern would affect the generation and accumulation of the primary and secondary metabolites, and eventually bring impact on the internal quality of traditional herb.[9–12] However, full investigation is still in vacancy, especially research on the cultivars from two major production areas in Anhui province (AH) and Inner Mongolia province (NM). In previous studies, eight platycosides contributed to differentiate four *Platycodi radix* cultivars,[13] and potential biomarkers from different parts of *Platycodon grandiflorus* were revealed by a nontargeted metabolome profiling,[14] but most focusing on triterpenoid saponins. A powerful approach was performed earlier this study, with 187 constituents were plausibly or unambiguously identified, including 85 triterpenoid saponins, 32 organic acid, 15 saccharides, 14 phospholipids, 8 flavonoids and 33 other compounds.[15] In addition, an analysis scheme of hydrophilic interaction liquid chromatography (HILIC) separation and tandem mass spectrometry combined with the online

[a]*School of Pharmacy, Fudan University, Shanghai, 201203, PR China*
[b]*NMPA Key Laboratory for Quality Control of Traditional Chinese Medicine, Shanghai Institute for Food and Drug Control, Shanghai 201203, PR China. E-mail: jishen2021@126.com*

† Electronic supplementary information (ESI) available. See DOI: 10.1039/d1ra08285j

‡ These authors contributed equally to this work.

Paternò–Büchi reaction was developed for the analysis of phospholipids in *Platycodi radix* in our laboratory, exposing the molecular species of phosphatidylcholine (PC), phosphatidylethanolamine (PE), lysophosphatidylethanolamine (LPE) and lysophosphatidylcholine (LPC).[15] Lipidomic studies on *Platycodi radix* have been rarely reported. As more categories of lipids tend to be found, further investigation is required for comprehensive lipid profile analysis of *Platycodi radix*.

Metabolome focuses on comprehensive analysis of metabolites in biological systems, which is consistent with the holistic thinking of traditional Chinese medicine.[16] Therefore, untargeted metabolome study is essential to deeply understand the inner quality and further improve the quality control of *Platycodonis radix*. As a vital category of metabolites, lipids are the major structural components of endomembranes and function as signaling molecules in biological systems.[17,18] Some lipids will be altered in response to adverse environmental conditions.[19] It provides a new point of view in supervising the component change in trends. In this study, a lipidome analysis based on reversed-phase liquid chromatography coupled with ion mobility-quadrupole time-of-flight mass spectrometry (RPLC-IM-QTOF-MS) was conducted aiming at the lipid of high content, which complemented the HILIC separation. *Platycodonis radix* from Taihe county in AH and Chifeng city in NM, which represent the major production regions in southern and northern planting areas in China, were collected and analyzed as the illustration. It was the first report that systematically compared both metabolome and lipidome differences between *Platycodonis radix* in two growing regions of China, providing vital information for the investigation of chemical composition in addition to platycosides.

2. Materials and methods

2.1. Chemicals and samples

LC/MS-grade water, acetonitrile and methanol were purchased from Merck KGaA (Darmstadt, Germany). LC/MS-grade formic acid was purchased from Thermo Fisher Scientific (Shanghai, China). Reference standards (i) deapioplatycodin D3, deapioplatycodin D, platycodin D2, polygalacin D, 1,1-diphenyl-2-picrylhydrazyl (DPPH) were provided by Yuanye bio-technology Co. Ltd (Shanghai, China). (ii) Lobetyolinin was purchased from A Chemtek Inc. (MA, USA). (iii) Nystose, lobetyolin and chlorogenic acid were got from national institutes for food and drug control (Beijing, China). *Platycodonis radix* used in this study, 12 samples from each origin, were collected form the local agricultural planting base of Taihe county in AH and Chifeng city in NM. All samples were authenticated based on the botany traits as recorded in *Flora of China* by Professor Yajun Cui (Shanghai University of Traditional Chinese Medicine) and the voucher specimen was deposited at the author's laboratory. Detailed information of these samples is provided in Table S1.†

2.2. Sample preparation

2.2.1. Metabolome sample preparation. An aliquot of 1.0 g fine powder of each *Platycodonis radix* sample was weighed, and 10 mL 70% (v/v) aqueous methanol was added. The methanol extract was subsequently prepared in an ultrasonic water bath for 30 min at room temperature and was centrifuged at 14 000 rpm. The supernatant was collected for further analysis. QC sample was obtained by equally mixed each test sample and served for the purpose of system real-time stability monitoring.

2.2.2. Lipidome sample preparation. 0.3 mL methanol and 1 mL MTBE were individually added to 50 mg fine powder of *Platycodonis radix*, which was then ultrasonically extracted for 10 min. The phase separation was induced by adding 0.25 mL water. After being centrifuged at 14 000 rpm for 10 min, the upper organic phase was collected and the lower phase was re-extracted with the same procedure. The extract was stored at −20 °C until analysis. 50 μL each test sample was pooled together to make the QC sample.

2.3. UPLC/IM-QTOF-MS conditions for metabolome and lipidome profiling

Metabolome profiling was performed by ACQUITY UPLC system coupled to Vion IMS-QTOF mass spectrometer (Waters Corporation, Milford, MA, USA) equipped with electrospray ionization (ESI) source. Chromatographic separation was carried out on a Waters CORTECS UPLC® T3 column (2.1 × 100 mm, 1.6 μm) at 40 °C. A binary mobile phase consisting of 0.1% aqueous formic acid (A) and acetonitrile (B) was programed as follows: 0.0–2.0 min, 0–0% B; 2.0–6.0 min, 0–23% B; 6.0–18.0 min, 23–25% B; 18.0–20.0 min, 25–50% B; 20.0–22.0 min, 50–55% B; 25.0–27.0 min, 70–100% B; 27.0–29.0 min, 100% B; and 29.1–33.0 min, 0% B. The flow rate was 0.5 mL min^{-1}, and the injection volume was 2 μL.

The MS was conducted in negative ion high-definition MS^E ($HDMS^E$) mode, and MS parameters were as follows: capillary voltage: 2.0 kV, sample cone voltage: 40 V, source offset voltage: 80 V, source temperature: 120 °C, desolvation temperature: 550 °C, low collision energy: 6 eV, high collision energy ramp: 20–80 eV, cone gas flow rate: 50 L h^{-1}, desolvation gas flow rate: 1000 L h^{-1}, and analyzer mode: sensitivity. Survey scan data were acquired from m/z 50 to 2000. Leucine enkephalin was used as the lock mass for both mass and collision cross section (CCS) calibration.

Lipid analysis was conducted on ACQUITY UPLC® CSH column (2.1 × 100 mm, 1.7 μm) at 55 °C with the flow rate of 0.4 mL min^{-1}. A binary mobile phase A was acetonitrile/water (60:40, v/v) with 5 mM ammonium formate and 0.1% formic acid, and B was isopropanol/acetonitrile (90:10, v/v) with 5 mM ammonium formate and 0.1% formic acid. Elution gradients was optimized as follows: 0.0–2.0 min, 40–43% B; 2.0–2.1 min, 43–50% B; 2.1–12.0 min, 50–54% B; 12.1–18.0 min, 54–70% B; 12.1–18.0 min, 70–99% B, 18.1–20.0 min, 40% B. The injection volume was 2 μL. Data acquisitions were per-formed in both positive and negative modes. The MS conditions were the same as above, with high collision energy ramp 20–40 eV was an exception.

2.4. Assay on total saponins

The content of total saponins in *Platycodonis radix* was determined according to the method described in European Pharmacopoeia 10.0.

2.5. Assay on oligosaccharides

An aliquot of 0.25 g powder of each *Platycodonis radix* sample was weighed accurately and extracted with 25.0 mL of 60% ethanol under ultrasonic conditions for 15 min. Allow to cool. Weigh the stopper conical flask accurately and make up the lost weight with 60% ethanol. Shake the flask and then filter through a membrane filter (nominal pore size 0.45 μm). Nystose was accurately weighed and dissolved with 60% methanol to prepare stock solution. The stock solution was further diluted to produce a series of standard solutions for calibration curves.

All analyses were performed on an Agilent Series 1260 system (Agilent Technologies, Santa Clara, CA, USA), equipped with evaporative light-scattering detector (ELSD).

Chromatographic separation was conducted on a Waters XBridge™ HILIC column (4.6 mm × 250 mm, 5 μm). A binary mobile phase consisting of water (A) and acetonitrile (B) was programmed in gradient as follows: 0.0–1.0 min, 88% B; 1.0–10.0 min, 88–78% B; 10.0–20.0 min, 78–65% B, 20.0–20.1 min, 65–88% B; 20.1–35 min, 88% B. The flow rate was 1.0 mL min^{-1}, and the injection volume was 5 μL. The temperature of the column oven was set as 30 °C. The evaporator temperature was set to 45 °C and the gas flow was set to 1.6 mL min^{-1}.

Establish a calibration curve with the common logarithm of the concentration (μg mL^{-1}) of reference solutions (corrected by the assigned percentage content of nystose) as the abscissa and the common logarithm of the corresponding peak area as the ordinate. Identify the peaks due to 7 oligosaccharides by relative retention, which shall be within ± 5% of the specified value. Check the relative retention as follow: GF2 = 0.85, GF3 (nystose) = 1.00, GF4 = 1.13, GF5 = 1.25, GF6 = 1.36, GF7 = 1.45, GF8 = 1.53. Calculate the percentage content of oligosaccharides, expressed as nystose, by taking the sum of the percentage contents of GF2-8.

2.6. Antioxidant activity

The antioxidant activity of *Platycodonis radix* from different origins was roughly compared by DPPH radical scavenging activity. The experiment was carried out according to the method of Wang *et al.* with slight modifications.[20] Briefly, the metabolome sample mentioned in 2.2.1. was diluted twice with 70% methanol, of which accurately measure 0.5 mL and mixed with 5 mL DPPH methanol solution (0.10 mM). Well stirred and allow the reaction under root temperature in the dark for 30 min. The absorbance was measured at 516 nm as A_{sample}. Take 0.5 mL 70% methanol and mixed with 5 mL DPPH methanol solution (0.10 mM), followed by the same procedure to obtain A_0. Take 0.5 mL diluted metabolome sample and mixed with 5 mL methanol, followed by the same procedure to obtain A_{ground}. The calculation of DPPH radical scavenging capacity is as follow:

$$\text{DPPH scavenging effect } (\%) = \left(1 - \frac{A_{sample} - A_{ground}}{A_0}\right) \times 100\%$$

2.7. Data analysis

Raw data of metabolome and lipidome profiling were imported into the Progenesis QI 2.1 software (Waters Corporation, Milford, CT, USA) for processing. SIMCA v14.1 software (Umetrics, Umea, Sweden) was applied for principal component analysis (PCA) and orthogonal partial least squares discriminant analysis (OPLS-DA). Heatmaps visualizing the relative concentration trends of potential chemical markers was obtained on the web server statistical analysis MetaboAnalyst 5.0 (https://www.metaboanalyst.ca/). Other data were analyzed using the statistical software Prism version 8.0 (GraphPad Software, Inc., La Jolla, CA, USA).

3. Results and discussion

3.1. Metabolome differences of *Platycodonis radix* in different growing regions

In the previous work, we compared different solvent extractions (Fig. S1†). Considering the number and abundance of peaks, 70% methanol was selected as the extraction solvent for metabolome sample. An untargeted component analysis by UPLC-IM-QTOF-HDMS^E acquisition under negative ion mode was utilized to obtain the metabolic profiles of *Platycodonis radix*. The MS data was then automatically processed by Progenesis QI that integrated with the functions of peak alignment, peak picking, ion fusion, deconvolution and normalization.[21] The obtained data matrix was handled according to the "30% rule in QC samples" and "80%" rule in test samples before multivariate statistical analysis with SIMCA.[22] Unsupervised PCA and supervised OPLS-DA models were performed to investigate the metabolite variations of *Platycodonis radix*. PCA score plot (Fig. 1A) showed grouping trends between samples from AH and NM, and natural grouping was achieved with $R^2X = 0.905$, $Q^2 = 0.641$, suggesting a significant difference in metabolome profiles between the two groups. QC samples were well-gathered, which indicated a statable UPLC QTOF-HDMS^E acquisition system was guaranteed. OPLS-DA model was applied to explore the potential metabolic markers that contributed most to the differences between two growing origins. The result exhibited that obvious group separation was observed with $R^2X = 0.653$, $R^2Y = 0.989$ and $Q^2 = 0.954$ (Fig. 1B). The high values of R^2 and Q^2 highlighted the well fitness and predictability of the OPLS-DA model. It was obviously to see that 24 samples were all within the ellipse in the model plane which defined as the 95% critical limit of the Hotelling T^2. In addition, 200 permutations were carried out to validate the model, and the intercepts were got with $R^2 = (0, 0.471)$ and $Q^2 = (0, -0.664)$ (Fig. 1C). All the values on the left were lower than the original point on the right, and the intercept of the regression line of the Q^2-points with the vertical axis was less than zero, implying that the model was not overfitted. *S*-plot (Fig. 1D) visualized the divergence brought on by the potential chemical markers. Variables with larger variable importance of projection (VIP)

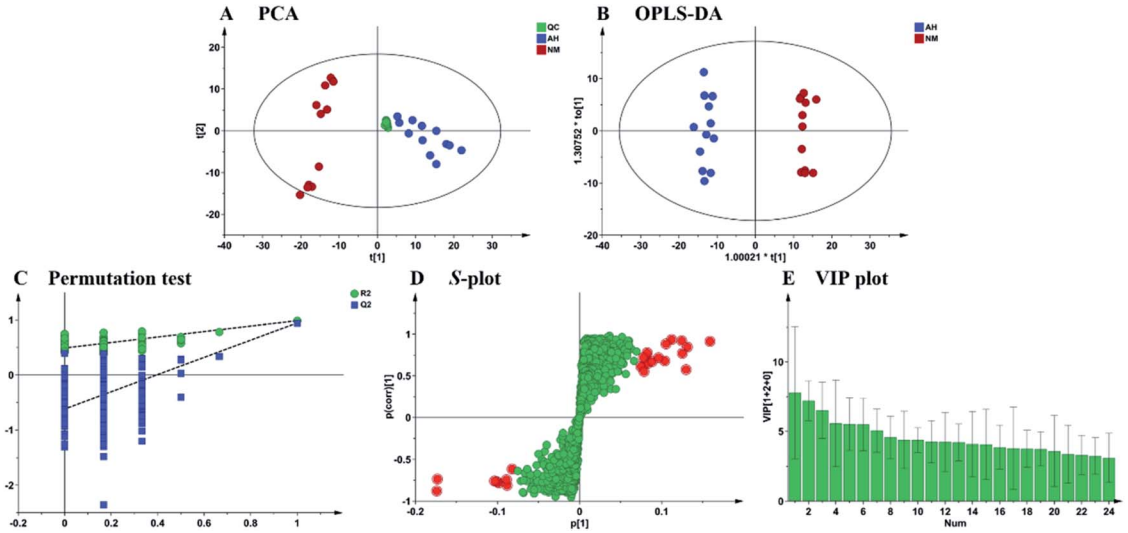

Fig. 1 Multivariate statistical analysis of the metabolites in *Platycodonis radix* from different geographical origins. (A) PCA score plot, $R^2X = 0.905$ and $Q^2 = 0.641$; (B) OPLS-DA score plot, $R^2X = 0.653$, $R^2Y = 0.989$ and $Q^2 = 0.954$; (C) permutation test of the established OPLS-DA model; (D) *S*-plot; (E) VIP plot.

values contributed more to distinguishing the two groups. 24 metabolic features with VIP > 3.0 (Fig. 1E) and $p < 0.05$ (Student's *t*-test) were selected as potential chemical markers. Hence, a list of potential metabolic markers was summarized (Table 1) and tentatively identified by querying to the *in house* library established in earlier study.[15]

Chromatographic and mass spectrometry information such as retention time (t_R), exact mass, isotope pattern and especially MS/MS fragmentation pattern was taken into consideration for structural annotation. The MS fragmentation behavior of compound **1** (t_R 11.82 min, *m*/*z* 1207.58), 5 (t_R 1.16 min, *m*/*z* 665.21), 10 (t_R 4.55 min, *m*/*z* 353.09) and 15 (t_R 22.70 min, *m*/*z* 452.28) in Table 1 were demonstrated in Fig. 2. Compound **1**, identified as polygalacin D, was one of the three major saponins from *Platycodonis radix* cultivated in China[23] and contributed the most significance in the model. Combined elimination of the apiosyl, xylosyl, rhamnosyl and arabinosyl sugar attached at C-28 rendered the feature ions at *m*/*z* 665.39 ($[M - H–Api–Xyl–Rha–Ara]^-$) and a series of diagnostic ions of sugar residues at *m*/*z* 541.18 ($[C_{21}H_{33}O_{16}]^-$), *m*/*z* 469.16 ($[C_{18}H_{29}O_{14}]^-$) and *m*/*z* 409.16 ($[C_{16}H_{25}O_{12}]^-$). The fragmentation pathway of compound **5** (*m*/*z* 665.21) was illustrated by the loss of H_2O and the gradual elimination of $C_6H_{10}O_5$ bringing on the ions of *m*/*z* 485.15 $[M - H–H_2O–C_6H_{10}O_5]^-$, 341.11 $[M - H–2C_6H_{10}O_5]^-$, 323.10 $[M - H–H_2O–2C_6H_{10}O_5]^-$, and 179.06 $[M - H–3C_6H_{10}O_5]^-$. Diagnostic ions at *m*/*z* 161.02 $[caffeoyl–H–H_2O]^-$ and 135.04 $[caffeoyl - H–CO_2]^-$ indicated that compound **10** was a typical caffeoylquinic acid. Product ion at *m*/*z* 191.06 of high intensity was caused by the loss of caffeoyl. A further neutral loss of H_2O to generate ion at *m*/*z* 173.05. Unknown phosphorous compound **15** was speculated to be a phospholipid with the elemental composition of $C_{21}H_{44}NO_7P$. Trace evidence of the diagnostic ion at *m*/*z* 214.05 and 196.04, representing the loss of the choline polar head $[C_5H_{13}NO_6P]^-$ and the ketene $[C_5H_{11}NO_5P]^-$. The loss of the fatty acid rendered the feature ion of *m*/*z* 255.23.[24]

The metabolic markers that explain the diversity from AH and NM root samples were 9 triterpenoid saponins, 5 saccharides, 5 phospholipids, 3 organic acids and 2 polyacetylenes. In order to systematically evaluate the differential metabolites, heatmap was used to visualize relative content trends of each potential metabolic markers in all test samples. Shade of colors represents different content of the metabolite. The redder or greener the color, the higher or lower the content. As shown in Fig. 3, the contents of these 24 markers varied a lot with different geographic origins. A higher abundance of triterpenoid saponins was observed in AH samples, while *Platycodonis radix* from NM tented to be rich in primary metabolites such as saccharides and lipids. Triterpenoid saponins, as one of the major secondary metabolites, were reported to be capital pharmacological active components in *Platycodonis radix*.[5,25] The results suggested that environmental conditions in Anhui province might induce the enhancement of triterpenoid saponins in *Platycodonis radix*, or might be conducive to the accumulation of these compounds.

3.2. Lipidome profiling of *Platycodonis radix*

A notable lipid MS intensity was observed in 70% methanol extract of *Platycodonis radix*.[15] The large structural diversity and broad polarity of lipids make the lipidomic analysis a significant challenge, for less-studied herbal derived lipids, it seems twice as difficult. To fully clarify these components, a lipidome methyl *tert*-butyl ether (MTBE) extraction method was utilized.[26,27] Lipid extraction is vital for lipid coverage, lipidomic data set quality and reported results. Comparative study had been launched and result showed that MTBE extraction possessed the advantages of broad lipid coverage, high MS response, more ion feature, good recovery, safety, operation

Table 1 Information of 24 potential metabolic markers for *Platycodonis radix* from different growing regions

No.	Compound ID	VIP value	Adducts	Formula	Mass error/ppm	MS/MS information	Identify	Classification
1[a]	11.82_1208.5822*n*	7.80	$[M-H]^-$	$C_{57}H_{92}O_{27}$	−1.12	665.39, 541.18, 469.16, 409.16	Polygalacin D	Triterpenoid saponins
2[a]	10.93_1385.6227*m*/*z*	7.21	$[M-H]^-$	$C_{63}H_{102}O_{33}$	0.56	843.44, 541.18, 519.33, 469.16, 409.16	Platycodin D2	Triterpenoid saponins
3	3.26_1314.4321*n*	6.53	$[M+HCOO]^-$	$C_{48}H_{82}O_{41}$	−1.47	972.32, 827.27, 503.16, 341.11, 179.06	1,1,1,1,1,1-Kestooctaose	Saccharides
4	22.99_433.2363*m*/*z*	5.59	$[M-H]^-$	$C_{21}H_{39}O_7P$	1.01	279.23, 171.01, 152.99, 96.97, 78.96	LPA 18:2	Phospholipids
5	1.16_666.2214*n*	5.53	$[M+HCOO]^-$	$C_{24}H_{42}O_{21}$	−0.82	485.15, 341.11, 323.10, 179.06	Nystose	Saccharides
6	2.16_873.2720*m*/*z*	5.51	$[M+HCOO]^-$	$C_{30}H_{52}O_{26}$	−1.63	647.20, 503.16, 485.15, 341.11, 323.10, 179.06	1-Fructofuranosylnystose	Saccharides
7	3.32_990.3266*n*	5.07	$[M+HCOO]^-$	$C_{36}H_{62}O_{31}$	−1.68	809.26, 647.20, 485.15, 341.11, 323.10, 179.06	1,1,1,1-Kestohexaose	Saccharides
8	3.32_1152.3793*n*	4.57	$[M+HCOO]^-$	$C_{42}H_{72}O_{36}$	−1.41	971.31, 647.20, 342.11, 179.06	1,1,1,1,1-Kestoheptaose	Saccharides
9[a]	10.34_1137.5325*m*/*z*	4.40	$[M+HCOO]^-$	$C_{52}H_{84}O_{24}$	−0.35	681.39, 663.37, 519.33, 501.32, 457.33	Deapioplatycodin D	Triterpenoid saponins
10[a]	4.55_353.0874*m*/*z*	4.39	$[M-H]^-$	$C_{16}H_{18}O_9$	−0.82	191.05624, 173.05, 161.02485, 135.04542	Chlorogenic acid	Organic acids
11	15.62_329.2332*m*/*z*	4.26	$[M-H]^-$	$C_{18}H_{34}O_5$	−0.19	311.22, 229.14, 211.13, 193.12, 183.14	Tianshic acid	Organic acids
12	22.65_295.2279*m*/*z*	4.24	$[M-H]^-$	$C_{18}H_{32}O_3$	0.78	277.22, 233.23, 205.12, 195.14, 125.10	Coronaric acid	Organic acids
13	11.44_1370.6350*n*	4.22	$[M-H]^-$	$C_{63}H_{102}O_{32}$	−1.07	827.44, 665.39, 541.18, 503.34, 469.16, 441.34	Polygalacin D2	Triterpenoid saponins
14	22.81_540.3309*m*/*z*	4.09	$[M+HCOO]^-$	$C_{24}H_{50}NO_7P$	0.98	480.31, 255.23, 242.08, 224.07	LPC 16:0/0:0	Phospholipids
15	22.70_452.2782*m*/*z*	4.08	$[M-H]^-$	$C_{21}H_{44}NO_7P$	1.22	255.23312, 214.05, 196.03830	LPE 16:0/0:0	Phospholipids
16	10.83_1134.5450*n*	3.88	$[M+HCOO]^-$	$C_{54}H_{86}O_{25}$	0.15	1091.53, 983.48, 681.39, 663.37, 501.32	Platycoside C	Triterpenoid saponins
17	22.26_564.3309*m*/*z*	3.81	$[M+HCOO]^-$	$C_{26}H_{50}NO_7P$	0.56	504.31, 279.23, 242.08, 224.07	LPC 18:2/0:0	Phospholipids
18	10.20_1253.5800*m*/*z*	3.77	$[M-H]^-$	$C_{58}H_{94}O_{29}$	0.01	843.44, 825.43, 663.37562; 519.33, 471.31	Deapioplatycodin D2	Triterpenoid saponins
19[a]	6.70_396.1784*n*	3.76	$[M+HCOO]^-$	$C_{20}H_{28}O_8$	0.7	305.12, 215.11, 185.10, 159.08, 143.07, 89.04	Lobetyolin	Polyacetylenes
20	22.17_476.2785*m*/*z*	3.60	$[M-H]^-$	$C_{23}H_{44}NO_7P$	1.06	279.23, 214.05, 196.03810	LPE 18:2/0:0	Phospholipids
21	13.37_1222.5611n	3.37	$[M-H]^-$	$C_{57}H_{90}O_{28}$	−0.43	1131.52, 635.38, 541.18, 469.16, 409.13	16-Oxo-platycodin D	Triterpenoid saponins
22[a]	6.18_558.2313*n*	3.32	$[M+HCOO]^-$	$C_{26}H_{38}O_{13}$	0.08	467.18, 323.10, 221.07, 179.06, 161.05	Lobetyolinin	Polyacetylenes
23	11.21_1105.5065*m*/*z*	3.24	$[M-H]^-$	$C_{52}H_{82}O_{25}$	−0.17	995.45, 717.35, 695.37, 633.36, 485.29, 423.29	Platyconic acid C	Triterpenoid saponins
24[a]	7.69_1254.5874*n*	3.11	$[M+HCOO]^-$	$C_{58}H_{94}O_{29}$	−0.85	843.44, 681.38; 519.33, 471.31, 409.13	Deapioplatycodin D3	Triterpenoid saponins

[a] Identified with authentic standards.

simplicity and more environment-friendly.[27,28] Therefore, MTBE was used as the extraction solvent for lipid extraction in this study.

Chromatographic separation was conducted on a charged surface hybrid (CSH) C_{18} column based on the lipids' acyl chain length, and the number, position and geometry of double bonds. Representative chromatograms of lipid profile *via* UPLC/IM-QTOF-HDMSE analysis were showed in Fig. S2.† More classes of lipid were explored in the lipidome analysis. A total of 170 lipidome metabolites which fell into 3 categories including 18 subclasses were tentatively characterized under both negative and positive ion mode (Table S2†). Among the annotated lipid molecules, 55.9% were glycerophospholipids (GP), 31.2% were glycerolipids (GL), and the remaining 12.9% were sphingolipids (SL) (Fig. 4). GP were the dominant lipids in *Platycodonis radix* samples. It is usually believed that GP construct cell membranes and play a key role in maintaining cell homeostasis.[29] Evidence showed that dietary GP possessed beneficial effects on different diseases and symptoms, such as coronary heart disease, inflammation and cancer, and apparently without serious side effects.[30] For GP, phosphatidic acid (PA, 19), PC (18), PE (18), phosphatidylinositol (PI, 9), LPE (7),

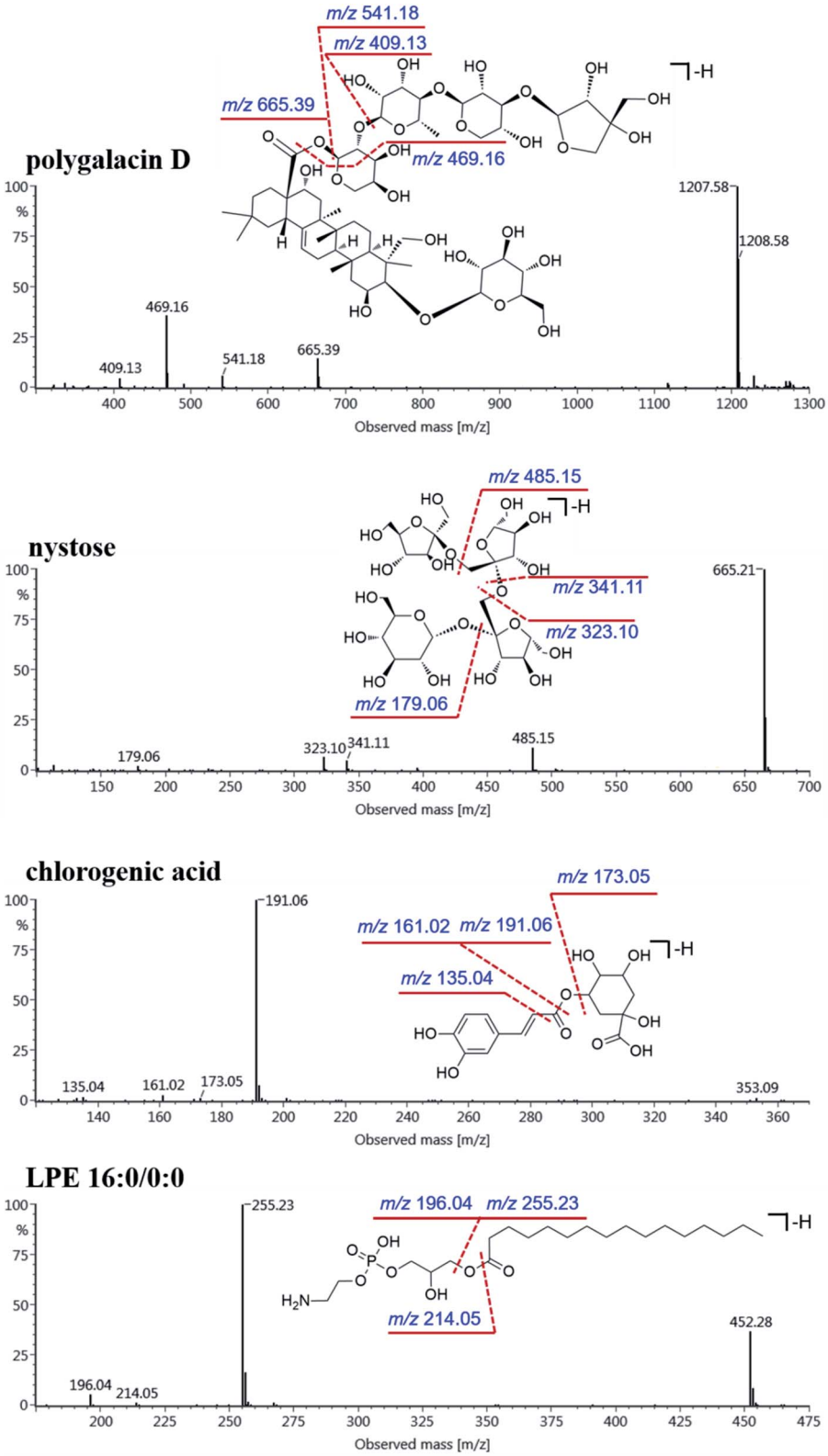

Fig. 2 Structural inference of typical metabolic markers in *Platycodonis radix* from different growing regions.

LPC (6), phosphatidylmethanol (PMeOH, 6), lysophosphatidic acid (LPA, 5), phosphatidylglycerol (PG, 3), lysophosphatidylinositol (LPI, 2) and phosphatidylserine (PS, 2) were identified. For SL, ceramide (Cer, 20) and hexosylceramide (HexCer, 2) were identified. For GL, diacylglycerol (DG, 8) and triacylglycerol (TG, 45) were identified.

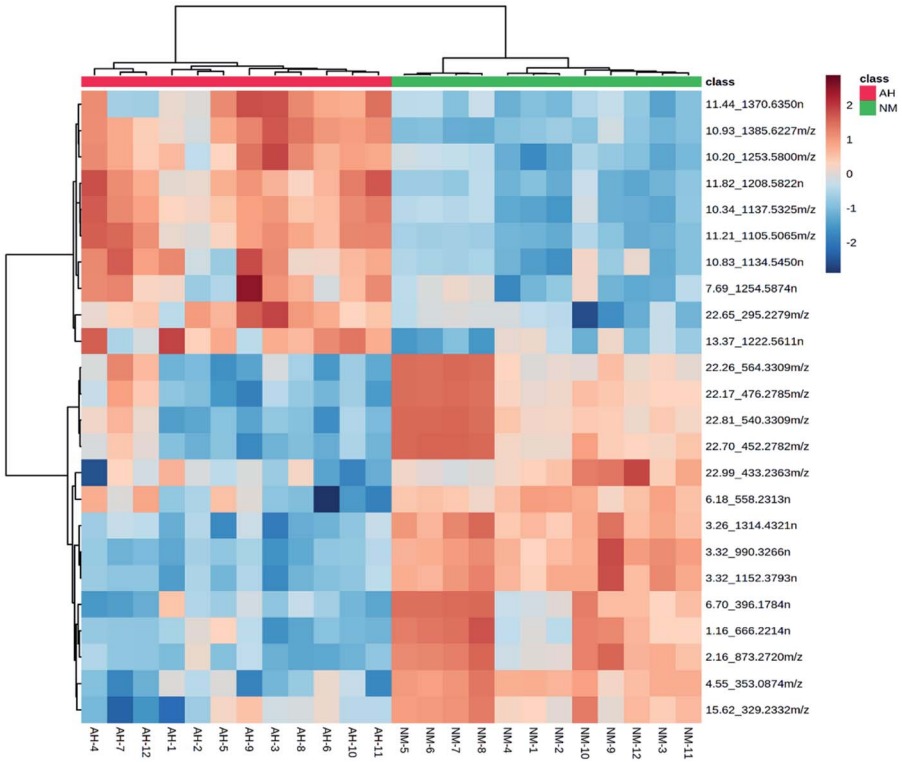

Fig. 3 Heatmap of the cluster analysis based on the abundance of 24 potential metabolic markers.

Structural elucidation of lipids was mainly based on the accurate molecular weight, elemental composition prediction, and fragmentation pathway. Although the MS intensity under positive ion mode exhibited higher, most phospholipids had neither characteristic fragments nor available fragments for fatty acyl identification. The negative ion mode provided more practical information for molecular structure recognition. The higher abundance of product ions generated by the collision-induced dissociation under the negative mode of phospholipids corresponded to the carboxylate anions and the loss of neutral fatty acid (FA) or ketene from the fatty acyl chains.[31] In this study, in negative ion mode, PC and LPC formed primarily $[M + HCOO]^-$ and the rest of the lipids tended to render $[M - H]^-$, while in the positive ion mode, TG formed primarily $[M + NH_4]^+$ and the rest of the lipids formed primarily $[M + H]^+$. Fig. 5 showed examples of *m/z* 671.47, 687.46, 802.56, 742.54, *m/z* 595.29, *m/z* 713.51, 894.75 and 654.60 for the samples.

PA, with the simplest polar head group, is a precursor and metabolite in the biosynthesis and catabolism of phospholipids.[24,31] A representative MS/MS fragmentation spectrum of PA 16:0/18:2 at *m/z* 671.47 was shown in Fig. 5A. Two dominant fragments were recognized as carboxylate anions at *m/z* 255.23 and 279.23, corresponding to FA 16:0 and 18:2, respectively. The observed signal at *m/z* 153.00 referred to the combined loss of

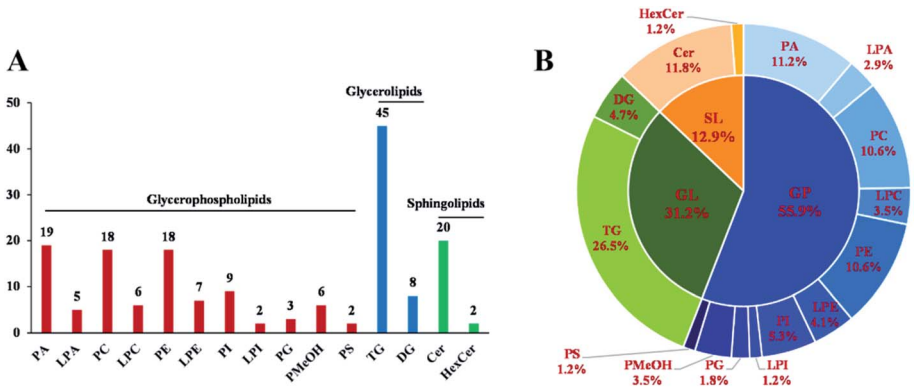

Fig. 4 Distribution of lipid subclasses identified in *Platycodonis radix*. Number of lipids in each subclass (A). Percentage composition of lipid subclasses identified in *Platycodonis radix* (B).

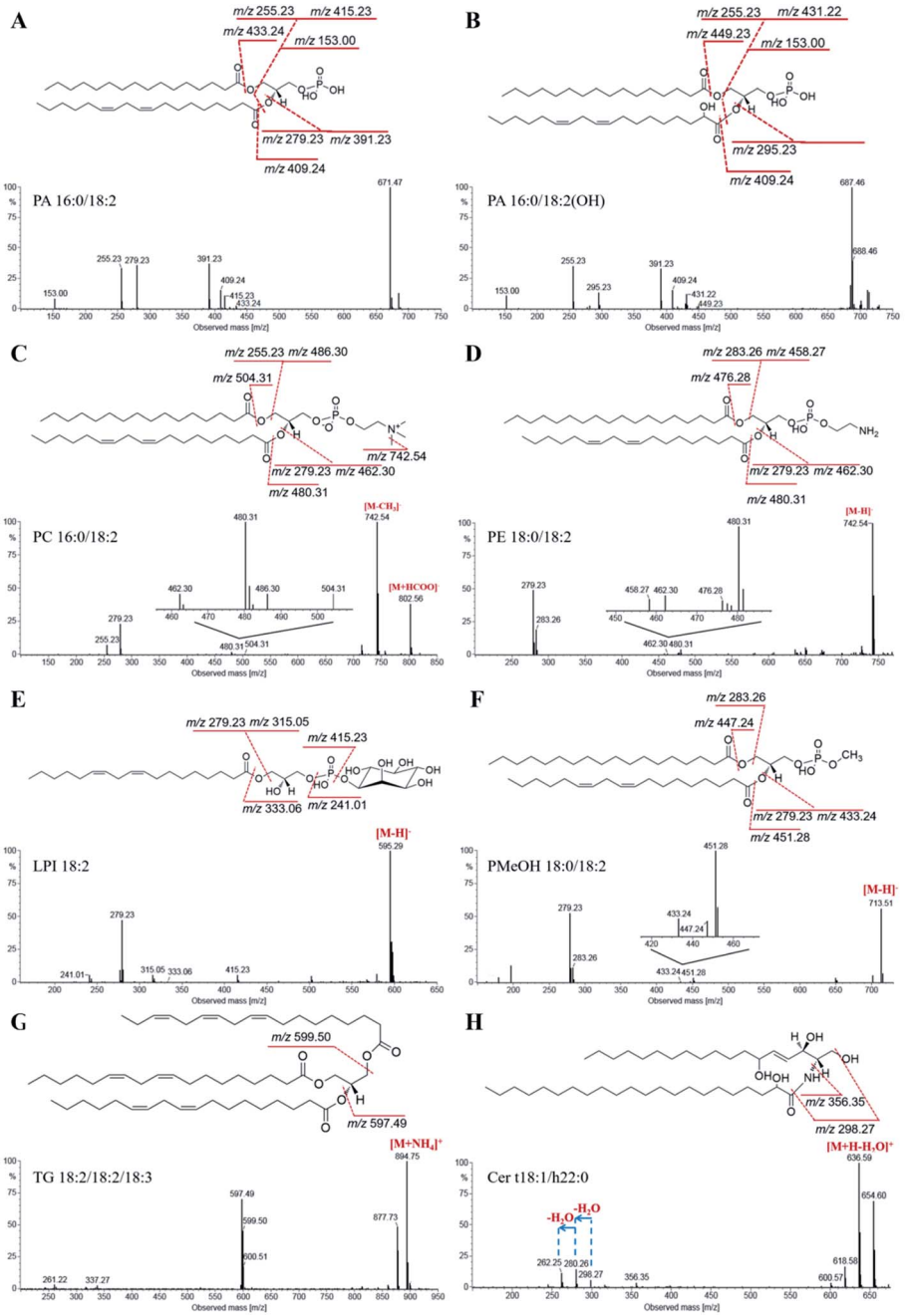

Fig. 5 Negative ion mode MS/MS spectra of PA 16:0/18:2 at *m/z* 671.47 (A), PA 16:0/18:2(OH) at *m/z* 687.46 (B), PC 16:0/18:2 at *m/z* 802.56 (C), PE 18:0/18:2 at *m/z* 742.54 (D), LPI 18:2 at *m/z* 595.29 (E), PMeOH 18:0/18:2 at *m/z* 713.51 (F); positive ion mode MS/MS spectra of TG 18:2/18:2/18:3 at *m/z* 894.75 (G) and Cer t18:1/h22:0 at *m/z* 654.60 (H).

two fatty acyl chains. The product ions in the middle of the spectrum were identified due to the neutral loss of fatty acyl moieties 16:0 (*m/z* 415.23 and 433.24) and 18:2 (*m/z* 391.23 and 409.24) either as FA or as ketenes, respectively. Since the detachment of fatty acyl moieties attached at sn-2 position was more favored than that in sn-1 (ref. 24) and to obtain corresponded FA or ketene,[32] *m/z* 671.47 was inferred to be PA 16:0/18:2. The most abundant PA at m/z 671.47 (PA 16:0/18:2), 695.47 (PA 18:2/18:2) and 652.59 (PA 18:2/18:3) were those lipids containing FA 16:0, FA 18:2 and FA 18:3 acyl chains. The presence of hydroxyl groups attached to fatty acyl chains was also observed. As shown in Fig. 5B, *m/z* 295.23 corresponded to the fatty acyl chain with a hydroxyl substituent on FA 18:2 (18:2(OH)). The signals at *m/z* 391.23, 409.24 and *m/z* 431.22, 449.23 were formed upon the detachment from the precursor ion of FA 18:2(OH) and 16:0 as neutral fatty acids or ketenes, respectively. The same strategy was applied to the identification of other phospholipid subclasses. PC are the major constituent of cell membranes in plants.[33] Fig. 5C presented the fragmentation pathway of PC 16:0/18:2 at *m/z* 802.56 as $[M + HCOO]^-$.

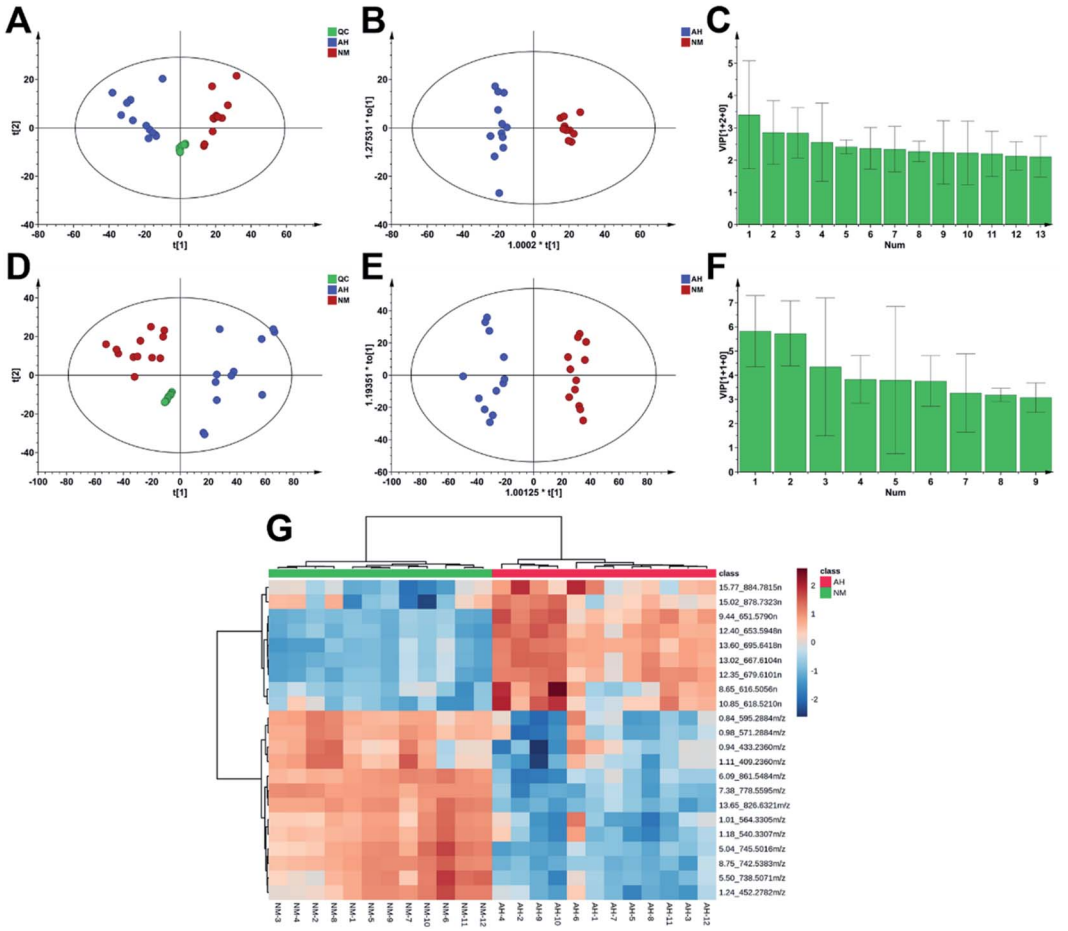

Fig. 6 PCA, OPLS-DA and VIP plot of AH and NM samples in negative mode (A–C) and positive mode (D–F). The statistical parameters as follows: (A) $R^2X = 0.838$, $Q^2 = 0.690$; (B) $R^2X = 0.721$, $R^2Y = 0.980$ and $Q^2 = 0.942$; (D) $R^2X = 0.902$, $Q^2 = 0.751$; (E) $R^2X = 0.626$, $R^2Y = 0.960$ and $Q^2 = 0.929$; heatmaps visualizing the intensities of potential chemical markers (G).

The fragment ion at m/z 742.54 $[M - CH_3]^-$ was due to the neutral loss of a methyl group from the choline moiety.[34] The MS/MS spectrum of the precursor ion at m/z 742.54 was recognized as PE 18:0/18:2 (Fig. 5D). The product ions at m/z 279.23 and 283.26 were straightly recognized as carboxylate anions of FA 18:2 and 18:0, respectively. The product ions at m/z 458.27 and 480.31 refer to the neutral loss of FA 18:2 as FA or as ketene, while the peak signals at m/z 458.27 and 476.30 were explained as due to the neutral loss of a fatty acyl chain 18:0 as FA or ketene, respectively. The regiochemistry PE 18:0/18:2 was inferred for m/z 742.54 based on relative intensity examination. Remarkably, the most abundant PC and PE at m/z 802.56 (PC 16:0/18:2), 826.57 (PC 16:0/18:2), 714.51 (PE 16:0/18:2) and 738.51 (PE 18:2/18:2) were mainly composed of fatty acyl chains 16:0 and 18:2. Lysophospholipids (LPL), modified phospholipids that lose one fatty acid by the phospholipases A catalyzed reaction, could be a potential compound that induce the remodeling of nutrient transport in the cell membrane and the proliferation of intestinal epithelial cells.[24,35] The fragmentation pathways of lysophospholipids (LPL) fell the same with that of their corresponding phospholipids. For LPI 18:2 at m/z 595.29 (Fig. 5E), m/z 279.23, 315.05 and 333.06 were related to the fatty acyl chain (FA 18:2). The product ions at m/z 415.23 was formed upon neutral loss of inositol from the precursor ion m/z 595.29. Still, m/z 241.01 was a characteristic fragment arose from the polar head group of this phospholipid subclass. The representative MS/MS spectrum of PMeOH yielded three fragment categories (Fig. 5F). m/z 179.11, 197.12 fragment ions were characteristic of the head group, m/z 279.23 and 283.26 corresponded to the detached fatty acids, m/z 433.24, 447.24 and 451.28 resulted from the loss of fatty acyl groups.

Fig. 5G illustrates the MS/MS spectrum of TG 18:2/18:2/18:3 at m/z 894.75 as $[M + NH4]^+$. m/z 877.73 was assigned to $[(M + NH_4)–NH_3]^+$. m/z 597.49 and 599.50. correspond to ions arose by the neutral loss FA 18:2 and FA 18:3, respectively. Based on the relative lower abundance of fragment ion $[M + H–R_2COOH]^+$ caused by the neutral loss of FA at the sn-2 position, it was possible to distinguish the regioisomers of TG molecules.[36,37] Cer and HexCer, as the essential structural components of the lipid bilayer of the cell membrane, play an important role in many cellular processes throughout the life cycle.[38] Sphingolipids contain a fatty acyl chain (FA), which is linked to a long chain base (LCB) through an amide bond.[39] FA moieties can be

Table 2 Information of 22 differential lipids for *Platycodonis radix* from different growing regions[a]

No.	Compound ID	VIP value	Adducts	Formula	Mass error/ppm	MS/MS information	Lipid species	Classification
1	9.44_651.5790*n*	5.82	$[M + H]^+$	$C_{40}H_{77}NO_5$	2.20	634.58, 616.57, 354.35, 298.27, 280.26, 262.25	Cer t18:1/h22:1	Sphingolipids
2	12.40_653.5948*n*	5.73	$[M + H]^+$	$C_{40}H_{79}NO_5$	−1.02	636.59, 618.58, 356.35, 298.27, 280.26, 262.25	Cer t18:1/h22:0	Sphingolipids
3	8.65_616.5056*n*	4.35	$[M + H]^+$	$C_{39}H_{68}O_5$	−1.98	599.50, 337.27, 263.22	DG 18:2/18:2	Glycerolipids
4	13.60_695.6418*n*	3.83	$[M + H]^+$	$C_{43}H_{85}NO_5$	−1.20	678.64, 660.63, 398.40, 316.28, 298.27, 280.26, 262.25	Cer t18:1/h25:0	Sphingolipids
5	15.77_884.7815*n*	3.80	$[M + NH_4]^+$	$C_{57}H_{104}O_6$	−2.30	603.53, 339.29, 265.25	TG 18:1/18:1/18:1	Glycerolipids
6	13.02_667.6104*n*	3.75	$[M + H]^+$	$C_{41}H_{81}NO_5$	−1.25	650.61, 632.61, 370.37, 298.27, 280.26, 262.25	Cer t18:1/h23:0	Sphingolipids
7	10.85_618.5210*n*	3.26	$[M + H]^+$	$C_{39}H_{70}O_5$	−1.18	601.52, 339.29, 337.27	DG 18:2/18:1	Glycerolipids
8	15.02_878.7323*n*	3.18	$[M + NH_4]^+$	$C_{57}H_{98}O_6$	−2.16	599.50, 337.27, 319.26, 263.24	TG 18:2/18:2/18:2	Glycerolipids
9	12.35_679.6101*n*	3.08	$[M + H]^+$	$C_{42}H_{81}NO_5$	−1.06	662.61, 644.60, 382.37, 298.27, 280.26	Cer t18:1/h24:1	Sphingolipids
10	0.94_433.2360*m/z*	3.41	$[M - H]^-$	$C_{21}H_{39}O_7P$	−0.64	279.23, 171.01, 153.00	LPA 18:2	Glycerophospholipids
11	1.11_409.2360*m/z*	2.86	$[M - H]^-$	$C_{19}H_{39}O_7P$	0.13	255.23, 171.01, 153.00	LPA 16:0	Glycerophospholipids
12	5.04_745.5016*m/z*	2.85	$[M - H]^-$	$C_{40}H_{75}O_{10}P$	−1.08	507.27, 489.26, 483.27, 465.26, 279.23, 255.23	PG 16:0/18:2	Glycerophospholipids
13	5.50_738.5071*m/z*	2.56	$[M - H]^-$	$C_{41}H_{74}NO_8P$	−0.10	476.28, 458.27, 277.22, 196.04, 140.01	PE 18:1/18:3	Glycerophospholipids
14	6.09_861.5484*m/z*	2.41	$[M - H]^-$	$C_{45}H_{83}O_{13}P$	−0.90	581.31, 577.28, 283.28, 279.23	PI 18:0/18:2	Glycerophospholipids
15	8.75_742.5383*m/z*	2.37	$[M - H]^-$	$C_{41}H_{78}NO_8P$	−0.89	480.31, 476.28, 462.30, 458.27, 283.26, 279.23	PE 18:0/18:2	Glycerophospholipids
16	0.84_595.2884*m/z*	2.34	$[M - H]^-$	$C_{27}H_{49}O_{12}P$	−0.93	415.23, 333.06, 315.05, 279.23, 241.01, 223.00	LPI 18:2	Glycerophospholipids
17	7.38_778.5595*m/z*	2.27	$[M + HCOO]^-$	$C_{40}H_{80}NO_8P$	−0.76	718.54, 480.31, 462.30, 255.23	PC 16:0/16:0	Glycerophospholipids
18	1.01_564.3305*m/z*	2.24	$[M + HCOO]^-$	$C_{26}H_{50}NO_7P$	−0.64	504.31, 279.23, 242.08, 224.07	LPC 18:2/0:0	Glycerophospholipids
19	1.24_452.2782*m/z*	2.22	$[M - H]^-$	$C_{21}H_{44}NO_7P$	0.60	255.23, 214.05, 196.04, 140.01	LPE 16:0/0:0	Glycerophospholipids
20	1.18_540.3307*m/z*	2.20	$[M + HCOO]^-$	$C_{24}H_{50}NO_7P$	0.22	480.31, 255.23, 242.08, 224.07	LPC 16:0/0:0	Glycerophospholipids
21	13.65_826.6321*m/z*	2.13	$[M - H]^-$	$C_{47}H_{90}NO_8P$	−0.60	564.40, 546.39, 476.31, 458.27, 367.56, 279.23	PE 24:0/18:2	Glycerophospholipids
22	0.98_571.2884*m/z*	2.11	$[M - H]^-$	C25H49O12P	−1.37	255.23, 241.01, 153.00	LPI 16:0	Glycerophospholipids

[a] Cer: ceramide; DG: diacylglycerol; TG: triacylglycerol; LPA: lysosphosphatidic acid; PG: phosphatidylglycerol; PE: phosphatidylethanolamine; PI: phosphatidylinositol; LPI: lysophosphatidylinositol; PC: phosphatidylcholine; LPC: lysophosphatidylcholine; LPE: lysophosphatidylethanolamine.

hydroxylated (OH) at various positions. For Cer t18:1/h22:0 (Fig. 5H), *m/z* 636.59, 618.58, 600.57 was attributed to successive dehydration of *m/z* 654.60. The *m/z* 298.27, 280.26 and 262.25 were used as markers for the saturated sphingoid base, while *m/z* 356.35 allowed direct identification of the FA moiety of Cer t18:1/h22:0.

3.3. Lipidome differences of *Platycodonis radix* in different growing regions

In order to visualize the grouping trends within the samples, a lipidome PCA model was constructed. Obvious group separation can be observed in both PCA score plots (Fig. 6A and D). In the supervised OPLS-DA mode (Fig. 6B and E), good fitness and predictability were represented by the values of $R^2X = 0.721$, $R^2Y = 0.980$, $Q^2 = 0.942$ (negative mode) and $R^2X = 0.626$, $R^2Y = 0.960$ and $Q^2 = 0.929$ (positive mode). VIP values were applied to discover potential markers (Fig. 6C and F). A total of 22 differential lipids molecular species were found, as summarized in Table 2. The relative content distributions of these markers in NM and AH samples were shown in the heatmap (Fig. 6G). Among them, 13 components displayed relatively higher contents in NM samples, while the rest 9 lipids were of higher contents in AH samples in general. Compared with AH samples, most *Platycodonis radix* form NM contained much higher level of GP. The annual temperature of NM is much lower than that of AH. It is reasonably speculated that the membrane should maintain the integrity and avoid intercellular damage in a much colder environment, which would bring the accumulation of GP in plants.[40] In contrast, AH samples possessed relatively higher levels of TG, DG and Cer than NM. Previous studies also have shown that the accumulation of ceramide might trigger the programmed cell death,[40,41] indicating that the maturity of *Platycodonis radix* in AH. As described above, the samples in AH accumulated more platycosides and showed higher maturity.

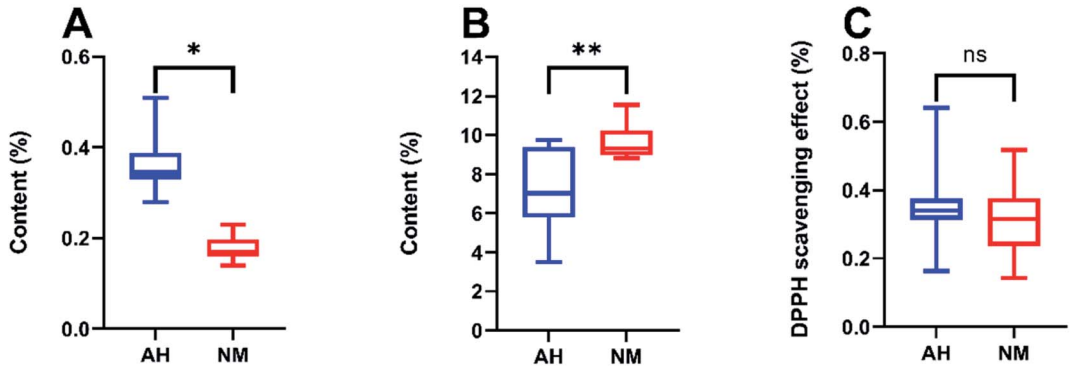

Fig. 7 Comparation of the total saponins (A), oligosaccharides (B) and the DPPH radical scavenging effect (C) in AH and NM samples. Data are presented as Mean ± SD ($n = 12$). *$p < 0.05$, **$p < 0.01$ and ns $p > 0.05$.

3.4. Comparation of the assays on total saponins and oligosaccharides

The contents of total saponins and oligosaccharides, which reflected the main quality differences, were determined subsequently. Representative chromatograms and linear calibration curves were provided in Fig. S3.† Results showed that the content of total saponins in AH samples was higher than that in NM samples (Fig. 7A). Conversely, higher content of oligosaccharides was observed in NM samples (Fig. 7B). The assays further verified the metabolic analysis results revealed in Section 3.1.

3.5. Comparation of the DPPH radical scavenging effect

The primary comparison of antioxidant activity, evaluated as DPPH radical scavenging effect, was conducted. Despite some differences in the chemical components, there was no significant difference in DPPH radical scavenging activity between AH samples and NM samples (Fig. 7C). This may be attributed to the fact that the antioxidant activity of *Platycodonis radix* samples is the result of the combined effect of multi-type constituents.

4. Conclusion

In the present study, integrated metabolome and lipidome profiling analysis were performed to investigate the spatial distribution of differential metabolites and lipids of *Platycodonis radix* in the two main growing areas of north and south China using UPLC-IM-QTOF-MS. The combination of QTOF-MS based data-acquisition and multivariable data-processing method would outperform traditional single variable analysis focusing on only one or one species of target compound, and unbiased conclusion was ready to come. Multivariate statistical analysis showed that there were significant differences in metabolome and lipidome profiles of the samples collected from two geographical origins (NM and AH) with distinct exogenous cultivating factors such as climate and soil. 24 differential metabolites and 22 differential lipids were tentatively characterized to exhibit the diversity of internal chemical composition from different origins. In addition, levels of specific components such as total saponins and oligosaccharides were determined, and the results were consistent with the trend of metabolome profiling. The introduction of comprehensive lipid analysis could clarify new orientation of the chemical profiling of medicinal food, and ultimately promote the reasonable application of *Platycodonis radix* as the health products and therapeutic drugs. Still, limitation of the study should be declared that the samples were all collected in single season. Further study is deemed necessary to investigate the seasonal variation in the metabolome and lipidome.

Conflicts of interest

The authors declare no conflict of interest.

Acknowledgements

This research was funded by the National Key R&D Program of China (No. 2017YFC1700800), Natural Science Foundation of Shanghai (No. 20ZR1450700) and Shanghai Sailing Program (No. 17YF1417100).

References

1 J. Lee, J. J. Cho, S. J. Hong, D. S. Kim, C. G. Boo and E. C. Shin, *J. Food Biochem.*, 2020, **44**, e13344.
2 C. Z. Wang, N. Q. Zhang, Z. Z. Wang, Z. Qi, B. Z. Zheng, P. Y. Li and J. P. Liu, *J. Mass Spectrom.*, 2017, **52**, 643–656.
3 M. Y. Ji, A. G. Bo, M. Yang, J. F. Xu, L. L. Jiang, B. C. Zhou and M. H. Li, *Foods*, 2020, **9**, 142.
4 J. W. Lee, S. H. Ji, G. S. Kim, K. S. Song, Y. Um, O. T. Kim, Y. Lee, C. P. Hong, D. H. Shin, C. K. Kim, S. E. Lee, Y. S. Ahn and D. Y. Lee, *Int. J. Mol. Sci.*, 2015, **16**, 26786–26796.
5 L. L. Zhang, M. Y. Huang, Y. Yang, M. Q. Huang, J. J. Shi, L. Zou and J. J. Lu, *Food Chem.*, 2020, **327**, 127029.
6 S. Lee, E. H. Han, M. K. Lim, S. H. Lee, H. J. Yu, Y. H. Lim and S. Kang, *J. Med. Food*, 2020, **23**, 1060–1069.
7 K. A. Hwang, Y. J. Hwang, P. R. Im, H. J. Hwang, J. Song and Y. J. Kim, *J. Med. Food*, 2019, **22**, 993–999.

8 W. Hao, Y. Shi, Y. Qin, C. Sun, L. Chen, C. Wu, Y. Bao and S. Liu, *Integr. Cancer Ther.*, 2020, **19**, 1534735420945017.
9 D. Wang, H. L. Koh, Y. Hong, H. T. Zhu, M. Xu, Y. J. Zhang and C. R. Yang, *Phytochemistry*, 2013, **93**, 88–95.
10 H. S. Peng, J. Wang, H. T. Zhang, H. Y. Duan, X. M. Xie, L. Zhang, M. E. Cheng and D. Y. Peng, *Chin. Med.*, 2017, **12**, 14.
11 H. H. Song, D. Y. Kim, S. Woo, H. K. Lee and S. R. Oh, *J. Ginseng Res.*, 2013, **37**, 341–348.
12 B. M. Huang, Q. L. Zha, T. B. Chen, S. Y. Xiao, Y. Xie, P. Luo, Y. P. Wang, L. Liu and H. Zhou, *Phytomedicine*, 2018, **45**, 8–17.
13 D. Y. Lee, B. R. Choi, J. W. Lee, Y. Um, D. Yoon, H. G. Kim, Y. S. Lee, G. S. Kim, Y. H. Lee and N. I. Baek, *Appl. Biol. Chem.*, 2019, **62**, 47.
14 C. Wang, N. Zhang, Z. Wang, Z. Qi, H. Zhu, B. Zheng, P. Li and J. Liu, *Molecules*, 2017, **22**, 1280.
15 W. Huang, H. Zhou, M. Yuan, L. Lan, A. Hou and S. Ji, *J. Chromatogr. A*, 2021, **1654**, 462477.
16 X. J. Wang, H. Sun, A. H. Zhang, W. J. Sun, P. Wang and Z. G. Wang, *J. Pharmaceut. Biomed.*, 2011, **55**, 859–868.
17 J. Hummel, S. Segu, Y. Li, S. Irgang, J. Jueppner and P. Giavalisco, *Front. Plant Sci.*, 2011, **2**, 54.
18 C. Barrero-Sicilia, S. Silvestre, R. P. Haslam and L. V. Michaelson, *Plant Sci*, 2017, **263**, 194–200.
19 B. Liu, X. Wang, K. Li and Z. Cai, *J. Agric. Food Chem.*, 2021, **69**, 8028–8037.
20 Y. J. Wang, W. Z. Huang, J. Z. Zhang, M. Yang, Q. C. Qi, K. M. Wang, A. Li and Z. X. Zhao, *RSC Adv*, 2016, **6**, 89338–89346.
21 H. Q. Pan, H. Zhou, S. Miao, D. A. Guo, X. L. Zhang, Q. Hu, X. H. Mao and S. Ji, *Chin. J. Nat. Med.*, 2021, **19**, 70–80.
22 M. Lv, J. Chen, Y. Gao, J. Sun, Q. Zhang, M. Zhang, F. Xu and Z. Zhang, *J. Sep. Sci.*, 2015, **38**, 3331–3336.
23 W. Li, Y. S. Sun, Z. Wang and Y. N. Zheng, *J. Liq. Chromatogr. R. T.*, 2012, **35**, 547–557.
24 C. D. Calvano, M. Bianco, G. Ventura, I. Losito, F. Palmisano and T. R. I. Cataldi, *Molecules*, 2020, **25**, 805.
25 E. Nyakudya, J. H. Jeong, N. K. Lee and Y. S. Jeong, *Prev. Nutr. Food Sci.*, 2014, **19**, 59–68.
26 X. Shi, W. Yang, S. Qiu, J. Hou, W. Wu and D. Guo, *J. Chromatogr. A*, 2018, **1548**, 64–75.
27 A. Gil, W. Zhang, J. C. Wolters, H. Permentier, T. Boer, P. Horvatovich, M. R. Heiner-Fokkema, D. J. Reijngoud and R. Bischoff, *Anal. Bioanal. Chem.*, 2018, **410**, 5859–5870.
28 A. Hu, F. Wei, F. Huang, Y. Xie, B. Wu, X. Lv and H. Chen, *J. Agric. Food Chem.*, 2021, **69**, 8964–8980.
29 M. P. Margutti, M. Reyna, A. C. Vilchez and A. L. Villasuso, *Environ. Exp. Bot.*, 2019, **158**, 150–160.
30 D. Kullenberg, L. A. Taylor, M. Schneider and U. Massing, *Lipids Health Dis*, 2012, **11**, 3.
31 L. Zhou, F. Yang, M. J. Zhao, M. H. Zhang, J. K. Liu and E. Marchioni, *Food Chem.*, 2021, 339.
32 M. Bianco, C. D. Calvano, L. Huseynli, G. Ventura, I. Losito and T. R. I. Cataldi, *J. Mass Spectrom.*, 2020, **55**, e4523.
33 W. van Nieuwenhuyzen and M. C. Tomas, *Eur. J. Lipid Sci. Tech.*, 2008, **110**, 472–486.
34 S. Song, L. Z. Cheong, H. Wang, Q. Q. Man, S. J. Pang, Y. Q. Li, B. Ren, Z. Wang and J. Zhang, *Food Chem.*, 2018, **240**, 1171–1178.
35 K. B. Jang, J. M. Purvis and S. W. Kim, *J. Anim. Sci.*, 2020, **98**, skaa227.
36 D. Jialin, X. Pei, H. Zhao, C. Gong and X. Xu, *J. Anal. Chem.*, 2020, **75**, 1024–1032.
37 T. Rezanka, I. Kolouchova, A. Cejkova, T. Cajthaml and K. Sigler, *J. Sep. Sci.*, 2013, **36**, 3310–3320.
38 D. C. Pant, S. Aguilera-Albesa and A. Pujol, *Neurobiol. Dis.*, 2020, 143.
39 J. Hartler, A. M. Armando, M. Trotzmuller, E. A. Dennis, H. C. Kofeler and O. Quehenberger, *Anal. Chem.*, 2020, **92**, 14054–14062.
40 L. L. Li, D. J. Wang, C. L. Sun, Y. Li, H. Lu and X. Wang, *J. Agr. Food Chem.*, 2021, **69**, 6710–6719.
41 Q. C. Hou, G. D. Ufer and D. Bartels, *Plant Cell Environ*, 2016, **39**, 1029–1048.